version: 2002 Mar 5

X-ray Detection of the Inner Jet in the Radio Galaxy 3C 129

D. E. Harris

Smithsonian Astrophysical Observatory, 60 Garden Street, Cambridge, MA 02138

H. Krawczynski

Yale University, P.O. Box 208101, New Haven, CT 06520-8101

and

G. B. Taylor

NRAO, Box O, Socorro NM 87801

ABSTRACT

During the course of an investigation on the interaction of the radio galaxy 3C 129 and its ambient cluster gas, we found excess X-ray emission aligned with the northern radio jet. The emission extends from the weak X-ray core of the host galaxy $\approx 2.5''$ to the first resolved radio knot. On a smaller scale, we have also detected a weak radio extension in the same position angle with the VLBA. Although all the evidence suggests that Doppler favoritism augments the emission of the northern jet, it is unlikely that the excess X-ray emission is produced by inverse Compton emission. We find many similarities between the 3C 129 X-ray jet and recent jet detections from Chandra data of low luminosity radio galaxies. For most of these current detections synchrotron emission is the favored explanation for the observed X-rays.

Subject headings: galaxies: active, individual(3C 129), jets—radiation mechanisms: non-thermal—radio continuum: galaxies—X-rays: galaxies

1. Introduction

The radio galaxy 3C 129 is a low luminosity (FRI type) 'tailed radio galaxy' seen in projection towards the outer edge of the X-ray emission from the hot gas of a nearby cluster of galaxies (Leahy and Yin, 2000). Since the cluster lies at low galactic latitude towards the anti-center, it has not been well studied in the optical.

We obtained Chandra observations in order to study the interaction of the radio structures with the hot intra cluster medium (ICM) and that work will be presented elsewhere (an analysis of the ICM properties has been performed by Krawczynski 2002, and a paper on pressure balance is in preparation). In this paper we report on faint X-ray emission detected from the core of the 3C 129 galaxy and from the inner 3 kpc of the northern radio jet. We include the results of 'follow-up' observations with the VLBA [1] in sec. 3.

X-ray emission from radio jets presents us with the problem of identifying the emission process but once this process is determined, we can then obtain new constraints on physical parameters (Harris and Krawczynski, 2002). With the introduction of the relativistic beaming model of Celotti (Celotti, Ghisellini, & Chiaberge, 2001) and Tavecchio (Tavecchio, et al. 2000), most X-ray emission from jets has been interpreted as indicating either synchrotron emission or inverse Compton scattering off the cosmic microwave background (CMB). For 3C 129, we show that synchrotron emission is the probable process, as has been found for a number of other FRI radio galaxies (Worrall, Birkinshaw, & Hardcastle, 2001; Hardcastle, Birkinshaw, & Worral 2001). The implications of the detected X-ray emission are discussed in sec. 5.

The redshift of the radio galaxy at the center of the cluster, 3C 129.1 is z=0.0208 (Spinrad, 1975) and we take this for our distance estimate of D_L=126 Mpc with $H_o = 50$ km s^{-1} Mpc^{-1} and $q_o = 0$. One arcsec then corresponds to 0.60 kpc.

2. X-ray data

The X-ray observation was obtained with the ACIS-S detector on the Chandra Observatory (obsid 2218, 2000Dec09). The exposure time was 31.46 ksec and the 3C 129 galaxy was observed with the back illuminated 'S3' chip. After standard Chandra pipeline processing (R4CU5UPD12.1 on 2000Dec12) we rejected intervals for which chip S5 had a count rate >1.8 c/s. This reduced the livetime to 30.403 ksec. Events with energies less than 0.3keV or greater than 8 keV were rejected.

We then binned the data by a factor of 1/4 to obtain images with pixel size 0.123″. Various Gaussian smoothing functions were then convolved with the data and one example

[1]The National Radio Astronomy Observatory is operated by Associated Universities, Inc., under contract with the National Science Foundation.

is shown in figure 1, an overlay of the radio image with X-ray contours. While it is clear that there is excess X-ray emission coincident with the first visible radio knot, 'N2.3', it appears that the X-ray morphology is essentially a projection from the core rather than a completely resolved separate structure. There is also a 1 to 2 σ excess located at the beginning of the second radio knot, 'N5.0'. All of these features are weak. For a circular aperture of radius $0.9''$, we find only 30 net counts in the core and an additional 12 net counts defining the jet. N5.0 contains only 4 net counts.

The observation was performed with a stage offset ('sim z') of -5.86mm ($119.5''$ or 243 pixels toward the readout edge), a y offset of $-1'$ to move the target to the center of a node, and a specified roll angle so as to position the 0.4° radio tail on the ACIS-S array. Since the target position was not the center of the galaxy, this procedure resulted in the core of the 3C 129 galaxy being $90''$ from the optical axis.

To check on the reality of the jet morphology, a 1.49keV point spread function (PSF) was generated to match the location off-axis and the pixel size of $0.123''$. This PSF image was then smoothed with a $1''$ Gaussian. The resulting image has quasi circular contours with radius of $0.66''$ for the 50% intensity levels. This value can be compared with $0.8''$ for 3C 129 in directions to the south and south-west (away from the jet) and $1.2''$ for the 50% contour in the position angle of the jet. If the X-ray jet were to be caused by statistical happenstance, it's alignment with the radio jet would be coincidental.

To asses the various emission mechanisms for the X-rays, we need to define areas (and their implied emitting volumes) and measure intensities. These regions were selected on the basis of the smoothed map (fig. 1), but the measurements were made on the event file. Mindful of the paucity of X-ray photons, we are content with order of magnitude estimates. For the core, we have taken a circle of radius $0.95''$; for the X-ray jet we use a rotated box of dimensions $2.03'' \times 1.63''$; and for the N5.0 feature we use a small circle of radius $0.92''$. These regions are shown in fig. 2.

Using the PIMMS tool and XSPEC/fakeit with a power law spectrum, we find a conversion value for 1 c/s (0.3 to 8 keV) to unabsorbed flux, f_x(0.5-5keV) of 1.11 (α=0.5); 1.16 (α=1.0); and 1.27 (α=1.5) $\times\ 10^{-11}$ erg cm^{-2} s^{-1}. This allows us to determine rough fluxes for the features measured.

3. Radio data

The VLA data used in this paper are those described in Taylor et al. (2001). However, we mainly used the 8 GHz data at their inherent resolution of $0.83''$ FWHM rather than the versions previously published which were smoothed to larger beams so as to match lower frequency data. This beam size is quite close to what we obtained with Chandra so meets the need of obtaining comparative morphologies and corresponding flux densities.

To obtain some sense of what role Doppler boosting might play near the radio core of 3C 129, on 16 December 2001 we observed the core at 4.986 GHz with the 10 element VLBA. Because of inclement weather, no data were obtained from the VLBA antenna at Mauna Kea. A total bandwidth of 32 MHz was recorded in left circular polarization only using 2 bit sampling. The VLBA correlator produced 16 frequency channels across each 8 MHz wide IF during every 2 second integration. Amplitude calibration for each antenna was derived from measurements of the antenna gain and system temperatures during each run. Delays, rates and phases were derived from the nearby (2.79 degrees distant) calibrator J0440+4244 and transferred to 3C 129. A 3 minute cycle of 120s:60s on target:calibrator was used. To check the quality of the phase referencing the calibrator J0427+4133 was observed 5 times during the 4 hour run. The coherence on J0427+4133 (2.58 degrees distant from J0440+4244) was found to be $\sim$85%.

Once delay and rate solutions were applied the data were averaged in frequency over 32 MHz. The data from all sources were edited and averaged over 20 second intervals using DIFMAP (Shepherd, Pearson & Taylor 1995) and then were subsequently self-calibrated and imaged. The final image is shown in Fig. 3. The position of the core of 3C 129 derived from modelfitting with DIFMAP is (J2000) RA 04h49m9.06396 DEC +45d00'39.342. Based on the observed offset of J0427+4133, the accuracy of this position should be $\sim$0.35 mas. The peak flux density is $\approx 2/3$ that obtained some years earlier with a $1.8''$ beam (Taylor et al. 2001).

The detection of the northern jet extending 6pc from the core supports the notion that the northern jet is the one coming towards us (in agreement with the VLA morphology) and that Doppler favoritism is operating on the pc scale. The PA of the 6pc scale feature is 13°; essentially the same as the value measured 630 pc from the core on the VLA map (PA $\approx 14^\circ$). Thus we may expect very little bending in the jet up to about 2kpc ($3.4''$) and this inner straight segment of the jet is the part that is detected by Chandra.

4. Parameters for Emission Models

To estimate physical parameters associated with various X-ray emission mechanisms, we need to assume values for some unmeasurable parameters such as the spectral index and refine volume estimates. We will also need to estimate the radio flux densities which correspond to the X-ray emitting volumes, not to the obvious radio features. For the radio spectral index we use $\alpha = 0.8$.

For the jet, we take a cylinder of length 1.8″ and radius 0.25″. For this volume, we ascribe a flux density of 3mJy at 8 GHz and f_x(0.5-5)= $\frac{12}{30403} \times 1.16\ 10^{-11} = 4.6\ 10^{-15}$ erg cm^{-2} s^{-1}. Since the X-ray emission is brighter towards the core end of this cylinder, and the radio is brighter at the down-stream end, this is a gross approximation.

4.1. Thermal Bremsstrahlung Emission

The log of the X-ray luminosity (0.5-5keV) for the jet is 39.967 (erg s^{-1}) and the density required to produce this emission from the cylindrical volume would be 0.7cm^{-3}. The mass of the emitting cylinder would be $1.4 \times 10^6\ M_\odot$. Assuming a temperature of 2 keV means that the pressure would be 4.4×10^{-9}dyne cm^{-2}. This pressure can be compared to that of the ICM at this location: 0.0075×10^{-9}dyne cm^{-2} (Krawczynski, 2002). Since this volume is well inside the galaxy, there could be additional pressure contributed by cooler gas which does not produce X-rays.

4.2. Synchrotron Emission

At similar resolutions, the X-ray emission decreases monotonically moving away from the core, whereas the radio brightness is low adjacent to the unresolved (0.83″ beam) core and then increases to the enhancement we call 'knot N2.3'. Because of this discrepancy in morphology, a simple synchrotron model is not easily constructed.

If the morphology difference arises by a statistical fluctuation from the small number of photons defining the X-ray jet, we may calculate the synchrotron parameters necessary to produce the observed X-rays. For the radio emission from N2.3 (10^7 to 10^{11} Hz), the log of the luminosity would be 39.517 and the equipartition field would be 40 μG. For a synchrotron X-ray model, we need to extend the radio spectrum up to 10^{18} Hz with the spectral index α=0.9. In this case the log of the luminosity would be 40.669 and the equipartition field would be 42 μG. Although there would be only an insignificant change in the total energy contained in the source, the power law distribution would have to extend to $\gamma = 7 \times 10^7$ with a halflife of some 60 years for electrons of this energy.

If the morphology difference is real, then the radio flux density to associate with the X-ray jet will be a factor of two or three less than the 3mJy found for knot N2.3. However, that would change the values derived above very little and the only different ingredient would be the natural picture of a quite limited region of shock acceleration capable of producing the high energies required for X-rays, followed by a further (downstream) segment of the jet where acceleration of the more common energies continues.

4.3. Inverse Compton Emission

The synchrotron self-Compton model fails because the photon energy density is so low that the predicted flux would be 4 orders of magnitude below that observed (assuming an equipartition field of 40 μG).

IC scattering off the CMB photons would require a magnetic field strength of 0.3 μG, more than a factor of 100 below the equipartition field and the emitting volumes appear not to coincide as expected from IC emission.

Even if we invoke relativistic beaming and ignore the disparity in morphology between radio and X-rays, to produce the observed X-ray jet would require an angle between the jet velocity vector and the line of sight of 7° or less and a beaming factor of 8. If there is a difference in morphologies, the beaming parameters become more stringent since the corresponding radio flux density to associate with the X-ray emission would be less than used in the calculations.

These values are inconsistent with estimates from the radio data. From the observed ratio of intensities of the inner radio jets (4.46), the angle between the line of sight and the N jet has to be less than 75° and is most likely greater than 30° since we see the two sides of the jet nowhere near lying on top of each other. This range in angles corresponds to beaming factors in the range 1.16 to 1.3 and jet fluid velocities, β (= $\frac{v}{c}$), in the range 0.3 to 1.

5. Discussion

Granted that we are dealing with few photons and thus an insecure morphology, we believe the evidence favors synchrotron emission for the observed X-rays. Undoubtedly there are bulk relativistic velocities in the jet producing the observed intensity differences between the N and S jets, but with velocity vectors not too far from the plane of the sky, we see only mild boosting and the parameters for IC/CMB emission are completely at odds with all other evidence.

If the bulk of the detected X-ray emission is in fact upstream of the radio knot N2.3, it would simply indicate that an acceleration region capable of producing γ of order 10^7 to 10^8

would be followed by a more extensive acceleration region incapable of such high energies, but rather producing up to $\gamma \approx 10^4$. Even in weak fields of order 30 to 50 μG, the half-life for electrons producing X-rays is so short that they could travel no more than 30pc from their acceleration region. Thus the X-rays clearly demarcate that sort of acceleration region.

There are now several detections of X-ray emission from jets in FRI radio galaxies. For M87 (Marshall et al. 2001) the radio, optical, and X-ray morphologies are quite close if not identical but upstream offsets of X-ray brightness peaks compared to those of the radio have been documented for 3C 66B (Hardcastle et al. 2001) and 3C 31 (Hardcastle et al. 2002). For these sources the offsets are a few hundred pc, slightly smaller than our (uncertain) value of 480pc for 3C 129. The situation in the jet of Cen A (Kraft et al. 2000) is confused with some features aligning well at radio and X-ray bands, but for others it is not always clear which features correspond at the other wavelength.

In Table 1 we give comparative values of size and luminosities for several FRI detections. It can be seen that the 3C 129 parameters are quite consistent with the others. While we cannot rule out thermal bremsstrahlung as the cause of the X-rays from 3C 129, it seems likely that as for the other FRI detections, synchrotron emission is the favored process.

This work was partially supported by NASA grants and contracts. At SAO: GO1-2135A and NAS8-39073; and at Yale: NAS8-39073 and GO 0-1169X.

References

Biretta, J.A., Stern, C.P., and Harris, D.E. 1991 AJ 101, 1632.

Hardcastle, M.J., Birkinshaw, M., & Worral, D.M. 2001 MNRAS 326, 1499 3c66B

Hardcastle, M.J., Worral, D.M., Birkinshaw, M., Laing, R.A. & Bridle, A.H. 2002, MNRAS (in press) 3C31

Harris, D. E. and Krawczynski, H. 2002 ApJ 565, 244

Kraft, R.P. et al. 2000 ApJ 531, L9

Krawczynski, H. 2002, ApJ (in press)

Leahy, D. A. and Yin, D. 2000, MNRAS 313, 617

Shepherd, M. C., Pearson, T. J., & Taylor, G. B. 1995, BAAS, 27, 903

Spinrad, H. 1975, ApJ 199, L1

Taylor, G.B., Govoni, F., Allen, S.A., & Fabian, A.C. 2001 MNRAS 326, 2

Worrall, D.M., Birkinshaw, M., & Hardcastle, M.J. 2001, MNRAS 326, L7

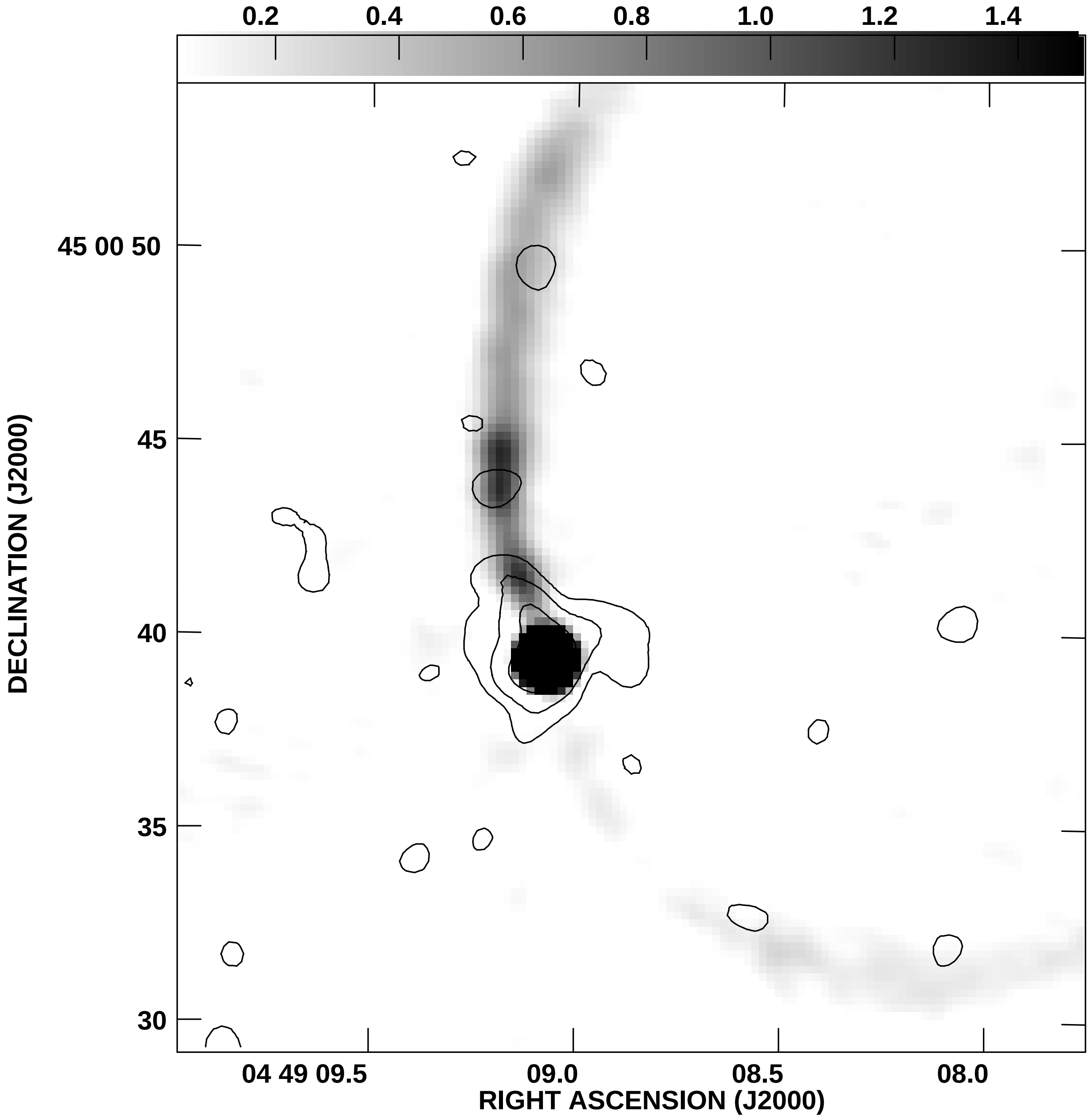

Fig. 1.— An 8 GHz VLA map (greyscale) of the inner part of 3C 129 with X-ray contours overlayed. The grey scale is from 0.05 to 1.5 mJy/beam and the beamwidth is 0.83″ FWHM. The X-ray data were smoothed with a Gaussian of FWHM=1″; contours are logarithmic, increasing by factors of 2 with the lowest contour at 2 counts per 0.123″ pixel. The X-ray image has been shifted 0.24″ in RA to align the radio and X-ray cores.

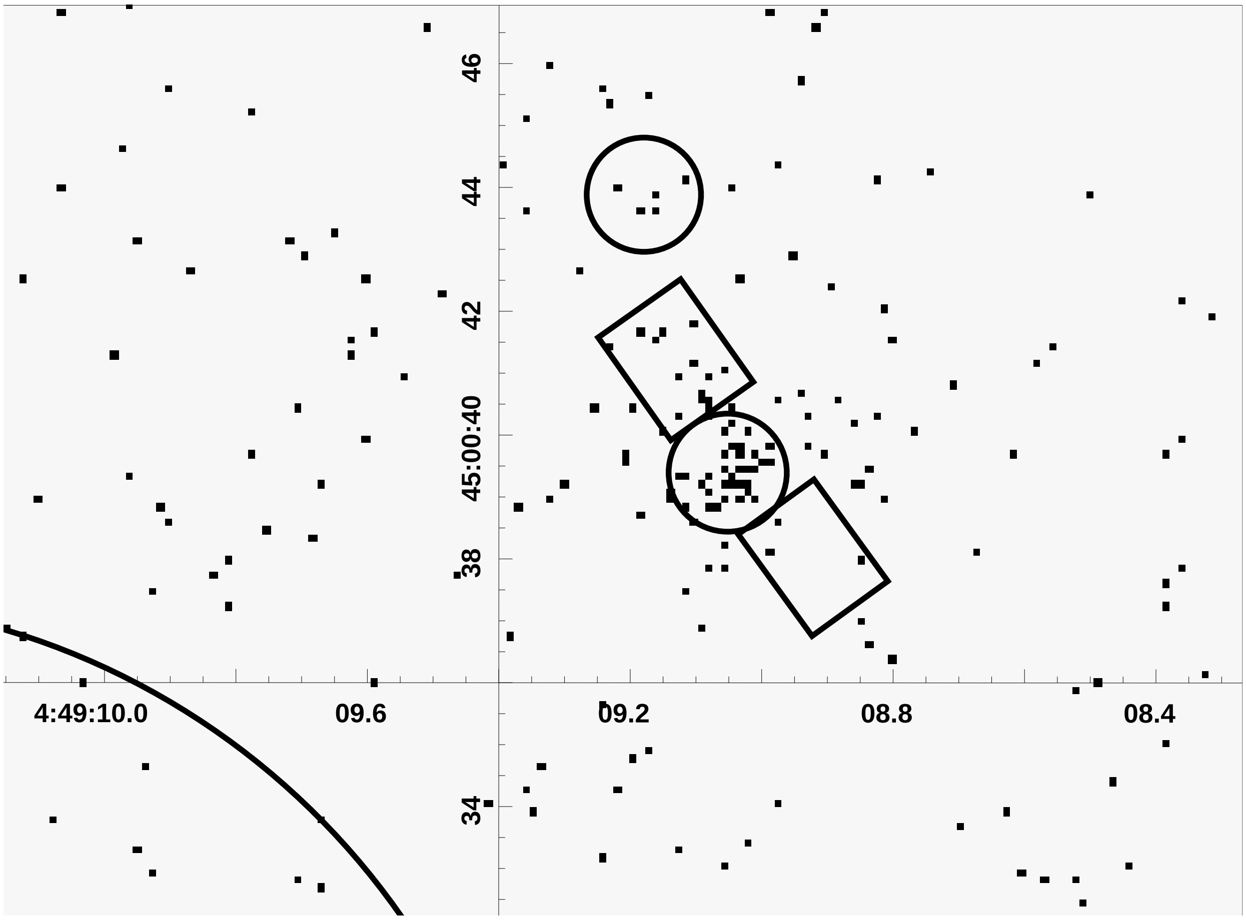

Fig. 2.— A map of the X-ray photons with the apertures chosen for intensity measurements overlayed. The segment of the large circle to the lower left is part of the circle used for background estimates. The circle with the obvious concentration of counts has a radius of $0.95''$ and serves to measure the core. The abutting rectangle to the NE is for the X-ray jet extending out to the N2.2 radio knot and the small circle beyond corresponds to the first part of the radio knot N5.0. The rotated box to the SW is a control region for the jet emission. We thank W. Joye for his work on the imaging tool, ds9 which allows us to make high quality figures with minimal effort.

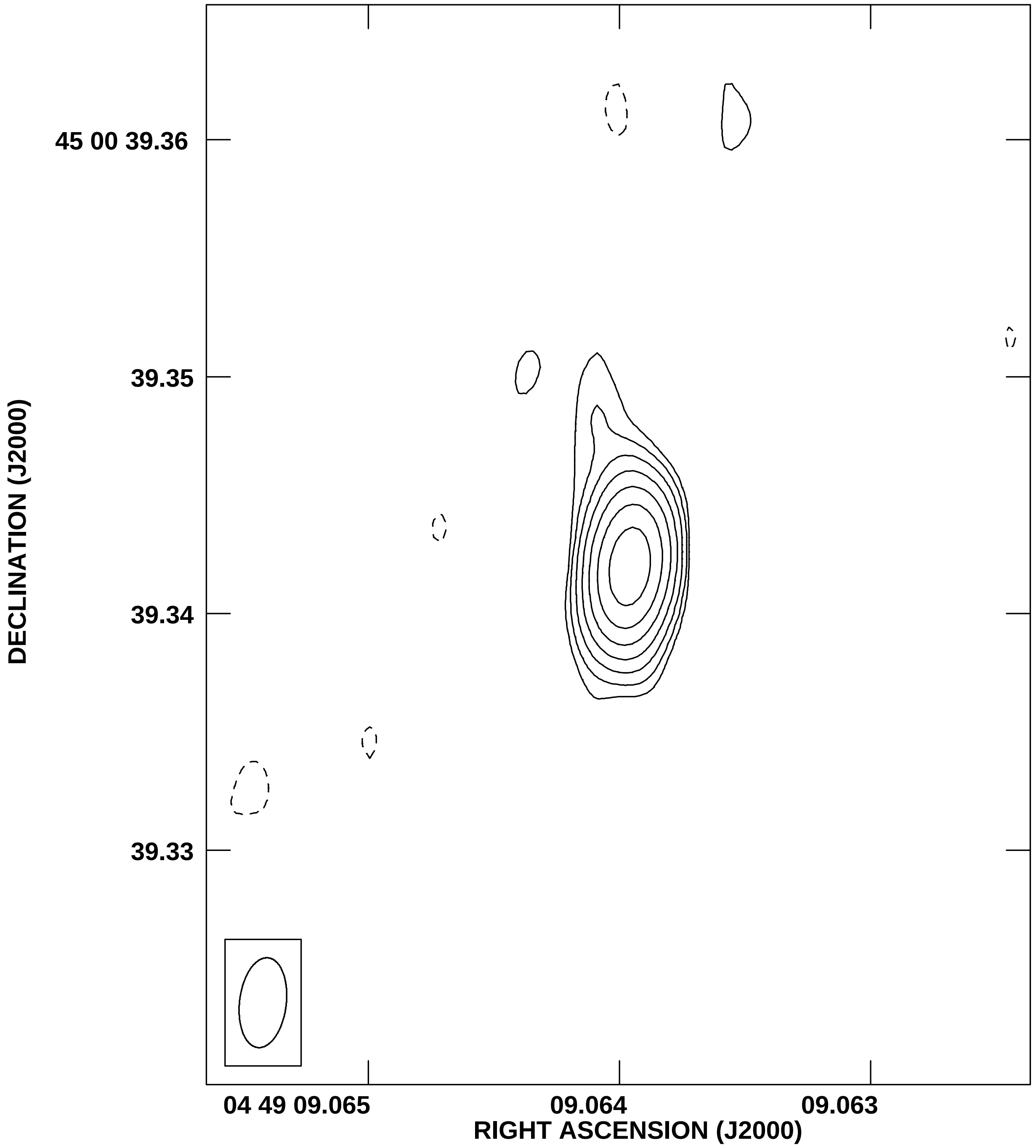

Fig. 3.— The VLBA 5GHz map. The beamwidth is 3.8 mas $\times$ 2.0 mas in PA=-8° and the contours are logarithmic, increasing by factors of 2 in brightness. The lowest contour is 0.25 mJy/beam and the peak intensity is 26.9 mJy/beam.

Table 1. Parameters for X-ray jets in FRI radio galaxies.

Source	Scale kpc/arcsec	Projected Length (pc)	L_x(0.5-5keV) 10^{40}erg s^{-1}	Reference
3C129	0.60	1320	0.9	this paper
3C31	0.48	3356	4.9	Hardcastle et al. 2002
B2 0206+35	1.02	2040	16.0	Worrall et al. 2001
3C66B	0.61	4270[a]	13.0	Hardcastle et al. 2001
B2 0755+37	1.17	2574	39.0	Worrall et al. 2001
M87	0.08	1386	7.8	Marshall et al. 2001
Cen A	0.02	3400	0.3	Kraft et al. 2000

[a]Most of the X-ray intensity is closer than 1220 pc from the core.